

Relativistic quantum-mechanical versus classical magnetic resonant scattering cross sections

N. A. Loudas^{1,2} N. D. Kylafis^{1,2} and J. E. Trümper³

¹ University of Crete, Department of Physics & Institute of Theoretical & Computational Physics, 70013 Herakleio, Greece

² Institute of Astrophysics, Foundation for Research and Technology-Hellas, 71110 Heraklion, Crete, Greece

³ Max-Planck-Institut für extraterrestrische Physik, Postfach 1312, 85741 Garching, Germany

Received ; accepted

ABSTRACT

Context. Radiative transfer calculations in strong (few $\times 10^{12}$ G) magnetic fields, observed in X-ray pulsars, require accurate resonant differential scattering cross sections. Such cross sections exist, but they are quite cumbersome.

Aims. Here we compare the classical (non-relativistic) with the quantum-mechanical (relativistic) resonant differential scattering cross sections and offer a prescription for the use of the much simpler classical expressions with impressively accurate results.

Methods. We have expanded the quantum-mechanical differential cross sections and kept terms up to first order in $\epsilon \equiv E/m_e c^2$ and $B \equiv \mathcal{B}/\mathcal{B}_{cr}$, where E is the photon energy and \mathcal{B}_{cr} is the critical magnetic field, and recovered the classical differential cross sections plus terms that are due to spin flip, which is a pure quantum-mechanical phenomenon.

Results. Adding by hand the spin-flip terms to the polarization-dependent classical differential cross sections, we find that they are in excellent agreement with the quantum mechanical ones for all energies near resonance and all angles. We have plotted both of them and the agreement is impressive.

Conclusions. We give a prescription for the use of the classical differential cross sections that guarantees very accurate results.

Key words. accretion – pulsars: general – stars: magnetic field – stars: neutron – X-rays: stars

1. Introduction

Cyclotron lines are prominent features in the spectra of X-ray pulsars. The first cyclotron line was discovered in Hercules X-1 (Trümper et al. 1977, 1978) and since then over 35 accreting magnetic neutron stars exhibit electron cyclotron lines, sometimes with harmonics (Staubert et al. 2019). They are also called cyclotron resonance scattering features (CRSFs).

Despite the many years that have passed since the first observation of a CRSF, it is still unclear where these features form and with what mechanism. Early on, it was suggested (Basko & Sunyaev 1976) that the CRSFs are produced in the radiative shock in the accretion column. However, no calculation has been done so far for the simultaneous production of the power-law spectrum and the cyclotron line in a radiative shock. Instead, several calculations have been performed using a slab, illuminated from one side (Ventura et al. 1979; Nagel 1981; Nishimura 2008; Araya & Harding 1999, Araya-Gochez & Harding 2000; Schoenherr et al. 2007).

Another interesting idea was given by Poutanen et al. (2013), who proposed that the CRSF is produced by reflection of the continuum emitted at the radiative shock on the surface of the neutron star. Again, no radiative transfer calculation has been reported yet on this mechanism.

A possible reason for the limited detailed calculations is the resonant differential cross sections. Not their unavailability, but their complexity. The expressions derived by Herold (1979), Daugherty & Harding (1986), Bussard et al. (1986), Harding & Daugherty (1991), Sina (1996), Gonthier et al. (2014), Mushtukov et al. (2016), and Schwarm (2017) for the complete, Quantum Electrodynamics, differential Compton resonant cross sections are quite general and, because of this, cumbersome and rather impractical. However, this generality is not needed in most cases.

Most of the cyclotron lines that have been observed so far (for a review see Staubert et al. 2019) are at cyclotron energies $E_c \ll m_e c^2$, implying magnetic fields $\mathcal{B} \ll \mathcal{B}_{cr}$, where $\mathcal{B}_{cr} = m_e^2 c^3 / e \hbar$ is the critical magnetic field. For such cases, an expansion of the full quantum mechanical cross sections up to first order in $\epsilon \equiv E/m_e c^2$ and $B \equiv \mathcal{B}/\mathcal{B}_{cr}$ gives simpler, but nevertheless accurate, expressions for the necessary calculations.

Known in the literature are the much simpler classical (Thomson) cross sections (Canuto, Lodenquai, & Ruderman 1971; Blandford & Scharlemann 1976; Nobili, Turolla, & Zane 2008a). The question then arises: can a prescription be found, such that the use of the simple classical cross sections in radiative transfer calculations gives very accurate results? The present work answers this question positively.

In § 2, we discuss the polarization-dependent cross sections. First, we give the classical ones. Then, we discuss the quantum-mechanical cross sections, that have been derived either with the Johnson & Lippmann (1949) wave functions or with the physically more meaningful Sokolov & Ternov (1968) formalism, and compare them numerically for $E \ll m_e c^2$ and $\mathcal{B} \ll \mathcal{B}_{cr}$. We expand to first order in the small parameters ϵ and B the cross sections given by Harding & Daugherty (1991) and Sina (1996). Finally, we offer a prescription with which the classical cross sections can be used for extremely accurate results. In § 3, we summarize our work.

2. The cross sections

2.1. Classical

The classical (Thomson) differential cross sections for polarized resonant scattering are given by Nobili, Turolla, & Zane (2008a; see also Canuto, Lodenquai, & Ruderman 1971; Blandford & Scharlemann 1976). After integrating over the azimuthal angle ϕ we have

$$\frac{d\sigma_{11}}{d\cos\theta'} = 2\pi \frac{3\pi r_0 c}{8} L(\omega, \omega_r) \cos^2 \theta \cos^2 \theta', \quad (1a)$$

$$\frac{d\sigma_{12}}{d\cos\theta'} = 2\pi \frac{3\pi r_0 c}{8} L(\omega, \omega_r) \cos^2 \theta, \quad (1b)$$

$$\frac{d\sigma_{21}}{d\cos\theta'} = 2\pi \frac{3\pi r_0 c}{8} L(\omega, \omega_r) \cos^2 \theta', \quad (1c)$$

$$\frac{d\sigma_{22}}{d\cos\theta'} = 2\pi \frac{3\pi r_0 c}{8} L(\omega, \omega_r), \quad (1d)$$

where the index 1 (2) stands for the ordinary (extraordinary) mode, r_0 is the classical electron radius,

$$L(\omega, \omega_r) = \frac{\Gamma/2\pi}{(\omega - \omega_r)^2 + (\Gamma/2)^2} \quad (2)$$

is the normalized Lorentz profile with $\omega = E/\hbar$ the photon frequency, $\omega_r = E_r/\hbar$ the resonant frequency, which in the non-relativistic regime is the cyclotron frequency $\omega_c = e\mathcal{B}/m_e c$, $\Gamma = 4e^2\omega_c^2/(3m_e c^3)$ accounts for the finite transition life-time of the excited state (e.g. Daugherty & Ventura 1978; Ventura 1979), and θ and θ' are the incident and scattered angles, respectively, with respect to the direction of the magnetic field $\vec{\mathcal{B}}$.

The polarization averaged differential cross section is given by

$$\frac{d\sigma}{d\cos\theta'} = 2\pi \frac{3\pi r_0 c}{16} L(\omega, \omega_r) (1 + \cos^2 \theta) (1 + \cos^2 \theta'). \quad (3)$$

2.2. Relativistic quantum mechanical

Expressions for the differential Compton scattering cross sections as functions of polarization, energy E , and magnetic field \mathcal{B} have been derived by Harding & Daugherty (1991), using the Johnson & Lippmann (1949) wavefunctions. Similar, but more accurate, expressions have been derived by Sina (1996) using the Sokolov & Ternov formalism (for a detailed discussion see Gonthier et al. 2014). At large values of \mathcal{B} , there are differences between the two (Schwarm 2017).

Since we are interested at non-relativistic energies and sub-critical magnetic fields, we compare numerically the expressions of Harding & Daugherty (1991) with those of Sina (1996) for $B = 0.03$. In Fig. 1, we compare $d\sigma_{11}/d\cos\theta'$ near resonance for four values of the incident angle θ with respect to the magnetic field, and four values of the scattered angle θ' . The black lines correspond to Harding & Daugherty (1991), while the red ones to Sina (1996). The curves essentially overlap, but for a detailed comparison *at resonance* we show in Fig. 2 the ratio of the two curves for the cases displayed in Fig. 1. The differences at resonance are less than 3%. We remark that similar agreement exists for the other three differential cross sections.

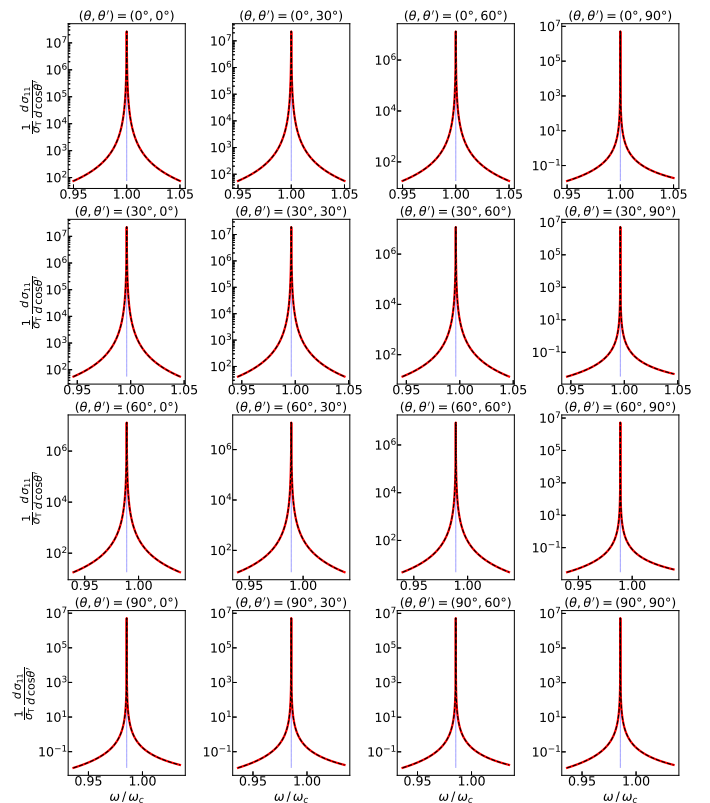


Fig. 1. Polarization-dependent differential cross section $(1/\sigma_T) d\sigma_{11}/d\cos\theta'$ as a function of photon energy $E = \hbar\omega$ for a set of incident angles θ and scattered angles θ' . The set of angles is 0, 30, 60, and 90 degrees, with θ changing vertically and θ' horizontally. The red solid lines are produced from the expression of Sina (1996), while the black dashed ones are produced from the expression of Harding & Daugherty (1991). In all cases, the resonant frequency is given by expression (7). The vertical line indicates the resonant frequency ω_r , which for $\theta \neq 0$ is smaller than ω_c . Here $E_c = \hbar\omega_c = 15.33$ keV.

In Fig. 3, we show in the form of heat maps the ratios *at resonance* of the differential cross sections calculated from the expressions of Harding & Daugherty (1991) to those of Sina (1996) for $B = 0.03$. It is evident that, for all incident angles θ and all scattered angles θ' , the ratio is between 1.000 and 1.027. Thus, for $B \ll 1$, it is irrelevant which of the two formalisms is used.

In order to find simpler expressions, that are nevertheless quite accurate for $E \ll m_e c^2$ and $\mathcal{B} \ll \mathcal{B}_{cr}$, we have

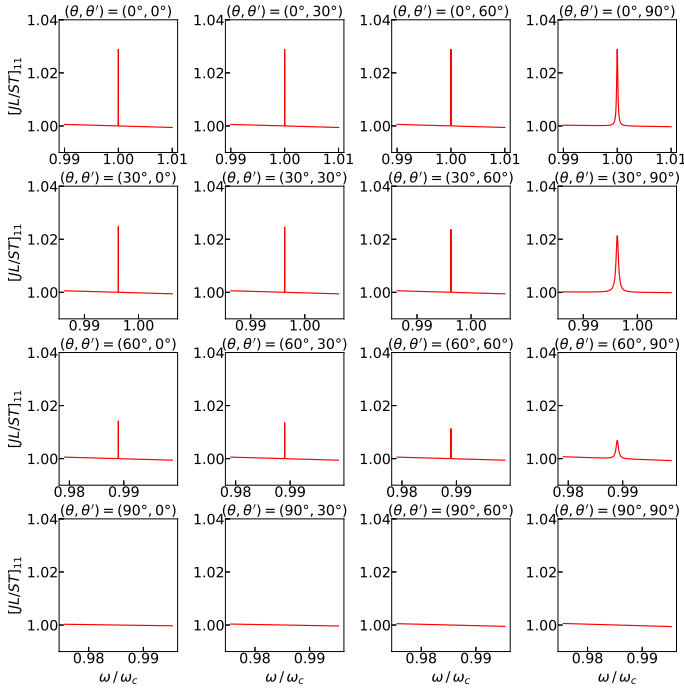


Fig. 2. Ratio of the Harding & Daugherty (1991) polarization-dependent differential cross section $(1/\sigma_T) d\sigma_{11}/d\cos\theta'$ to those of Sina (1996) for the cases shown in Fig. 1.

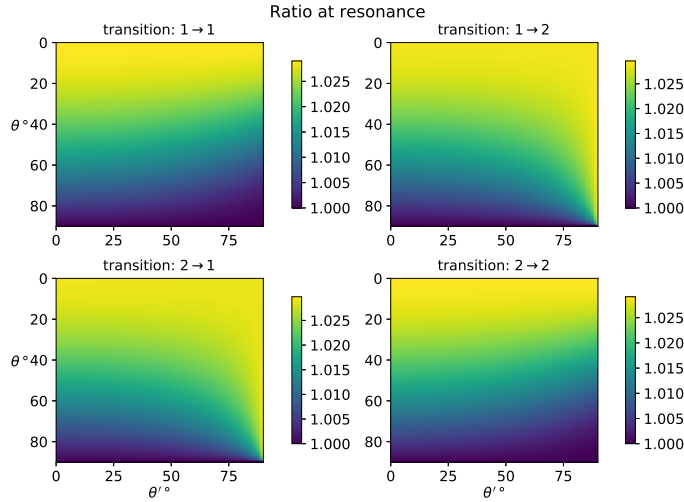


Fig. 3. Ratio of the Harding & Daugherty (1991) polarization-dependent differential cross sections at resonance to those of Sina (1996) for different incident and scattered angles θ and θ' , respectively. In all cases, the resonant frequency is given by expression (7) and $B = 0.03$.

expanded the expressions of Harding & Daugherty (1991) to first order in the small parameters $\epsilon = E/m_e c^2$ and $B = \mathcal{B}/\mathcal{B}_{cr}$. This is done in Appendix A. Here we give the results.

$$\frac{d\sigma_{11}}{d\cos\theta'} = 2\pi \frac{3\pi r_o c}{8} \left[g^{1 \rightarrow 1} \cdot L_- + h^{1 \rightarrow 1} \cdot L_+ + \sqrt{2B} \cos\theta \cos\theta' \frac{L_- \cdot L_+}{L_{mix}} \right], \quad (4a)$$

$$\frac{d\sigma_{12}}{d\cos\theta'} = 2\pi \frac{3\pi r_o c}{8} \left[g^{1 \rightarrow 2} \cdot L_- + h^{1 \rightarrow 2} \cdot L_+ + \sqrt{2B} \cos\theta \cos\theta' \frac{L_- \cdot L_+}{L_{mix}} \right], \quad (4b)$$

$$\frac{d\sigma_{21}}{d\cos\theta'} = 2\pi \frac{3\pi r_o c}{8} \left[g^{2 \rightarrow 1} \cdot L_- + h^{2 \rightarrow 1} \cdot L_+ + \sqrt{2B} \cos\theta \cos\theta' \frac{L_- \cdot L_+}{L_{mix}} \right], \quad (4c)$$

$$\frac{d\sigma_{22}}{d\cos\theta'} = 2\pi \frac{3\pi r_o c}{8} \left[g^{2 \rightarrow 2} \cdot L_- + h^{2 \rightarrow 2} \cdot L_+ + \sqrt{2B} \cos\theta \cos\theta' \frac{L_- \cdot L_+}{L_{mix}} \right], \quad (4d)$$

where $L_-(\omega, \omega_r)$, $L_+(\omega, \omega_r)$ and $L_{mix}(\omega, \omega_r)$ are the normalized Lorentz profiles, which are characterized by the decay widths Γ'_- , Γ'_+ , and Γ'_{mix} , respectively, and are given in Appendix A. The resonant frequency ω_r is given in eq. (7) below. In addition, $g^{s \rightarrow s'}$ (θ, θ', B) and $h^{s \rightarrow s'}$ (θ, θ', B) are first degree polynomials in B , and are given in Appendix A. Note that, s represents the polarization mode of the incident photon, whereas s' that of the scattered photon.

In Appendix B, we have expanded the expressions of Sina (1996) to first order in $\omega = E/(\hbar m_e c^2)$ and $B = \mathcal{B}/\mathcal{B}_{cr}$. The results are:

$$\frac{d\sigma_{11}}{d\cos\theta'} = 2\pi \frac{3\pi r_o c}{8} \left[\mathcal{G}^{1 \rightarrow 1} \cdot L_- + h^{1 \rightarrow 1} \cdot L_+ + \sqrt{2B} \cos\theta \cos\theta' \frac{L_- \cdot L_+}{L_{mix}} \right], \quad (5a)$$

$$\frac{d\sigma_{12}}{d\cos\theta'} = 2\pi \frac{3\pi r_o c}{8} \left[\mathcal{G}^{1 \rightarrow 2} \cdot L_- + h^{1 \rightarrow 2} \cdot L_+ + \sqrt{2B} \cos\theta \cos\theta' \frac{L_- \cdot L_+}{L_{mix}} \right], \quad (5b)$$

$$\frac{d\sigma_{21}}{d\cos\theta'} = 2\pi \frac{3\pi r_o c}{8} \left[\mathcal{G}^{2 \rightarrow 1} \cdot L_- + h^{2 \rightarrow 1} \cdot L_+ + \sqrt{2B} \cos\theta \cos\theta' \frac{L_- \cdot L_+}{L_{mix}} \right], \quad (5c)$$

$$\frac{d\sigma_{22}}{d\cos\theta'} = 2\pi \frac{3\pi r_o c}{8} \left[\mathcal{G}^{2 \rightarrow 2} \cdot L_- + h^{2 \rightarrow 2} \cdot L_+ + \sqrt{2B} \cos\theta \cos\theta' \frac{L_- \cdot L_+}{L_{mix}} \right], \quad (5d)$$

where $L_-(\omega, \omega_r)$, $L_+(\omega, \omega_r)$, $L_{mix}(\omega, \omega_r)$ and $h^{s \rightarrow s'}$ are the same as in (4a)-(4d), while the correction functions $\mathcal{G}^{s \rightarrow s'}$ are slightly different from the $g^{s \rightarrow s'}$ ones and are given in Appendix B. Note that, in order to avoid confusion between the different notations, we have employed the notation of Harding & Daugherty (1991) in eqs. (5) instead of the notation of Sina (1996) that we systematically use in Appendix B.

It is important to notice two things: a) The similarity of eqs. (5) with those of (4). They are identical, except for the small differences between g and \mathcal{G} . This, of course, is not surprising given the ratio plots in Fig. 2 and the heat plots in Fig. 3. b) The expressions in eqs. (4) and (5) are much simpler than the full expressions given by Harding & Daugherty (1991) and Sina (1996), respectively.

2.3. Even simpler expressions

Looking at expressions (4) and (5), we have wondered whether all the terms in them are crucial. Thus, we have written the extremely simple expressions that follow.

$$\frac{d\sigma_{11}}{d\cos\theta'} \approx 2\pi \frac{3\pi r_0 c}{8} \left(\cos^2\theta \cos^2\theta' \cdot L_- + \frac{B}{2} \cdot L_+ \right), \quad (6a)$$

$$\frac{d\sigma_{12}}{d\cos\theta'} \approx 2\pi \frac{3\pi r_0 c}{8} \left(\cos^2\theta \cdot L_- + \frac{B}{2} \cos^2\theta' \cdot L_+ \right), \quad (6b)$$

$$\frac{d\sigma_{21}}{d\cos\theta'} \approx 2\pi \frac{3\pi r_0 c}{8} \left(\cos^2\theta' \cdot L_- + \frac{B}{2} \cos^2\theta \cdot L_+ \right), \quad (6c)$$

$$\frac{d\sigma_{22}}{d\cos\theta'} \approx 2\pi \frac{3\pi r_0 c}{8} \left(L_- + \frac{B}{2} \cos^2\theta \cos^2\theta' \cdot L_+ \right). \quad (6d)$$

The terms proportional to L_- are identical to the classical cross sections (1), because L_- is equal to L given by eq. (2). The terms proportional to L_+ are non-classical, because they contain the decay width Γ_+ , which is associated with the spin flip.

In Fig. 4, we compare expression (6b) with expression (5b) for $B = 0.03$ and in Fig. 5, we present the ratio of these two formulae. The differences are impressively negligible. The same is true for the heat maps *at resonance* (Fig. 6).

For quick calculations with $B \ll 1$, where high accuracy is not demanded, one may safely use the very simple expressions (6), while for more accurate ones, expressions (5) are recommended. Of course, the highest accuracy is provided by the expressions of Sina (1996). It is our hope that these very simple expressions, together with the prescription that we give in the next subsection, will make resonant Compton scattering calculations easily doable.

2.4. The prescription

If, in a calculation, one wants to use the much simpler differential cross sections (1a) - (1d), then for accurate results the following prescription should be followed.

1) The spin-flip terms must be added by hand. Thus, eqs. (6a) - (6d) should be used. Of course, the exact results (5a) - (5d) are not that complicated.

2) For the resonant frequency ω_r , the relativistically correct expression

$$\omega_r = \frac{m_e c^2}{\hbar} \frac{2B}{1 + \sqrt{1 + 2B \sin^2\theta}} \quad (7)$$

should be used in the Lorentz profile (2) and not the cyclotron frequency $\omega_c = E_c/\hbar$.

3) In the classical (Thomson) limit, there is no change in the photon energy after scattering, i.e. $\epsilon' = \epsilon$. However, naturally there is an energy change (see § Appendix A) and the prescription dictates that the energy ϵ' of the photon after scattering should be taken equal to

$$\epsilon' = \frac{\epsilon^2 \sin^2\theta + 2\epsilon}{1 + \epsilon(1 - \cos\theta \cos\theta') + \sqrt{f_1(\epsilon, \theta, \theta') + f_2(\epsilon, \theta, \theta')}}}, \quad (8a)$$

where

$$f_1(\epsilon, \theta, \theta') = 1 + 2\epsilon \cos\theta'(\cos\theta' - \cos\theta), \quad (8b)$$

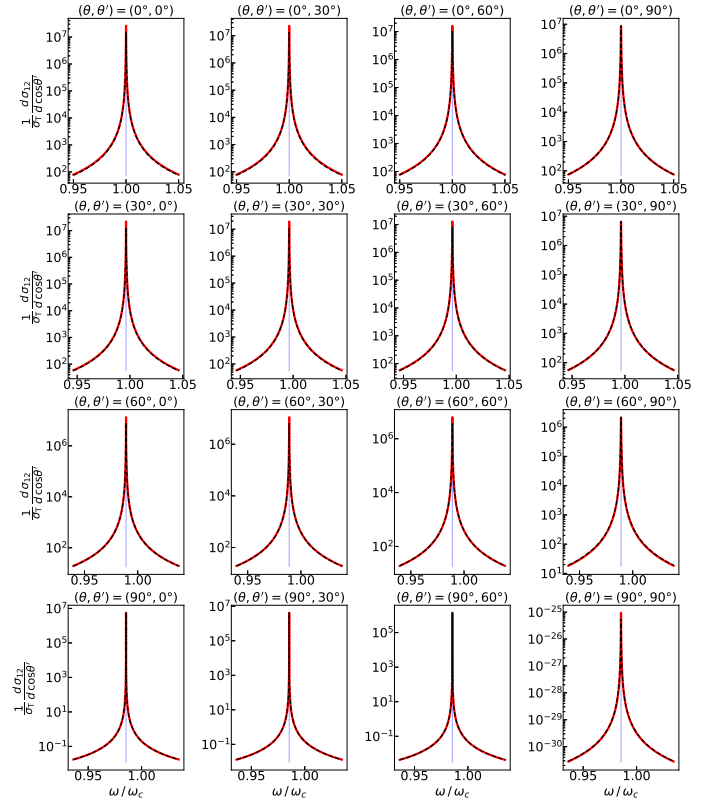


Fig. 4. Polarization-dependent resonant differential cross section $(1/\sigma_T) d\sigma_{12}/d\cos\theta'$ as a function of photon energy $E = \hbar\omega$ for a set of incident angles θ and scattered angles θ' . The set of angles is 0, 30, 60, and 90 degrees, with θ changing vertically and θ' horizontally. The red solid lines are produced from the first order expansion (5b) of Sina (1996), while the black dashed ones are produced from the simplified expression (6b). In all cases, the resonant frequency is given by expression (7). The vertical line indicates the resonant frequency ω_r , which for $\theta \neq 0$ is smaller than ω_c . Here $E_c = \hbar\omega_c = 15.33$ keV.

and

$$f_2(\epsilon, \theta, \theta') = \epsilon^2(\cos\theta - \cos\theta')^2. \quad (8c)$$

If the polarization of the CRSF is not of interest, then the polarization-averaged cross section can be used and it is

$$\frac{d\sigma}{d\cos\theta'} = 2\pi \frac{3\pi r_0 c}{16} (1 + \cos^2\theta)(1 + \cos^2\theta') \left[L_- + \frac{B}{2} \cdot L_+ \right]. \quad (9)$$

Note that for $B \ll 1$, the polarization-averaged cross section (3) is very accurate. No additional terms due to spin flip are necessary.

In this paper, we have restricted ourselves to cyclotron energies $E_c \lesssim 50$ keV, because most of the observed CRSFs are in this energy range (Staubert et al. 2019). However, a few CRSFs with $E_c > 50$ keV have been observed (Staubert et al. 2019), plus the recently reported (Ge et al. 2020) champion with $E_c = 90.32$ keV. For this reason, in Fig. 7 we compare the relativistically correct $d\sigma_{12}/d\cos\theta'$ ($\theta = 0, \theta' = \pi/2$) of Sina (1996) with the modified classical one (eq. 6b) for $E_c = 25$ keV (left panel), 50 keV (middle panel), and 100 keV (right panel). Clearly, 100 keV is not much less than $m_e c^2$. Nevertheless, we show it for the readers to

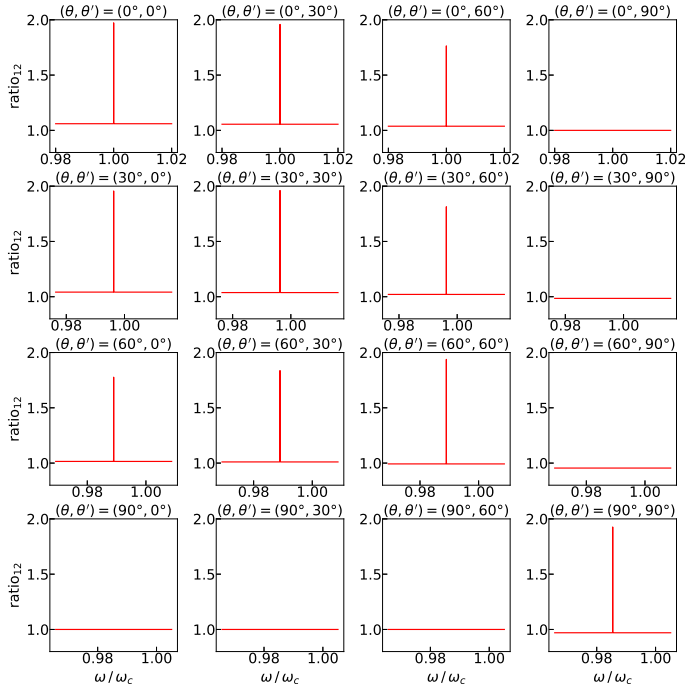


Fig. 5. Ratio of the polarization-dependent differential cross sections $d\sigma_{12}/d\cos\theta'$ given by (5b) to the simplified expression (6b) for the cases shown in Fig. 4.

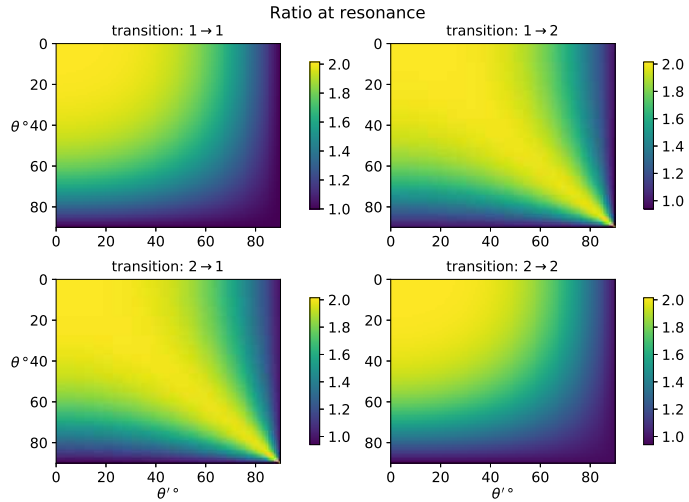


Fig. 6. Ratio at resonance of the exact polarization-dependent differential cross sections (5) to the approximate expressions (6) for different incident and scattered angles θ and θ' , respectively. In all cases, the resonant frequency is given by expression (7) and $B = 0.03$.

see the magnitude of the discrepancy between classical and quantum-mechanical cross sections.

3. Summary

We have shown numerically that, for photon energies $E \ll mc^2$ and magnetic field strengths $\mathcal{B} \ll \mathcal{B}_{cr}$, the relativistic polarization-dependent resonant differential cross sections of Harding & Daugherty (1991), derived with the Johnson & Lippmann (1949) wave functions, are in excellent agree-

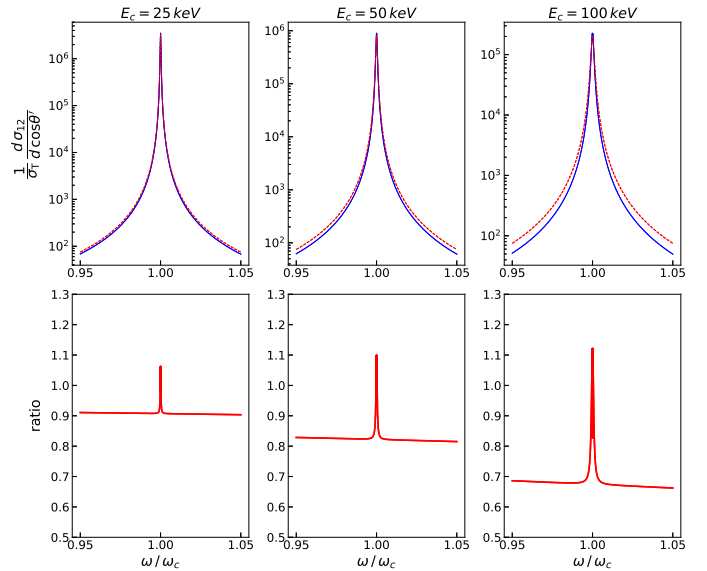


Fig. 7. *Top panels:* Comparison of the relativistically correct $d\sigma_{12}/d\cos\theta'$ ($\theta = 0, \theta' = \pi/2$) from Sina (1996) (blue solid line) with the modified classical one (eq. 6b) (red dashed line) for $E_c = 25$ keV (left panel), 50 keV (middle panel), and 100 keV (right panel). *Bottom panels:* Corresponding ratios of the curves shown in the top panels

ment with the ones of Sina (1996), derived with the Sokolov & Ternov (1968) formalism.

We have shown analytically that the expansion up to first order in $\epsilon = E/m_e c^2$ and $B = \mathcal{B}/\mathcal{B}_{cr}$ of the expressions of Harding & Daugherty (1991) and of Sina (1996) lead to nearly identical results.

We have provided simple, heuristic, but very accurate, expressions for the polarization-dependent resonant differential cross sections, together with a prescription that should be followed, for easy to perform detailed calculations involving resonant scattering at $E_c \lesssim 50$ keV.

Acknowledgements. We thank an anonymous referee for pointing out to us the Sokolov & Ternov (1968) formalism. We also thank Roberto Turolla and Alexander Mushtukov for useful discussions concerning the Sokolov & Ternov (1968) formalism. We are indebted to Alice Harding for sending us the unpublished PhD Thesis of Ramin Sina and to Peter Gonthier for e-mail exchanges. N.D.K. would like to thank Sterl Phinney for his notes on the classical magnetic scattering cross sections.

References

- Araya, R., & Harding, A. 1999, ApJ, 517, 334
- Araya-Góchez, R., & Harding, A. 2000, ApJ, 544, 1067
- Baring, M. G., Gonthier, P. L., & Harding, A. K. 2005, ApJ, 630, 430
- Basko, M. M., & Sunyaev, R. A. 1976, MNRAS, 175, 395
- Blandford, R. D., & Scharleman, E. T. 1976, MNRAS, 174, 59
- Bussard, R. W., Alexander, S. B., Meszaros, P. 1986, Phys. Rev. D, 34, 440
- Canuto, V., Lodenguai, J., & Ruderman, M. 1971, Phys. Rev. D, 3, 2303
- Daugherty, J. K., & Harding, A. K. 1986, ApJ, 309, 362
- Daugherty, J. K., & Ventura, J. 1978, Phys. Rev. D, 18, 1053
- Ge, M. Y., Ji, L., Zhang, S. N. et al. 2020, ApJ, in press
- Gonthier, P. L., Baring, M. G., Eiles, M. T., Wadiasingh, Z., Taylor, C. A., & Fitch, C. J. 2014, PhysRevD, 90, 043014
- Harding, A. K., & Daugherty, J. K. 1991, ApJ, 374, 687
- Herold, H. 1979, Phys. Rev. D, 19, 2868
- Herold H., Ruder H., & Wunner G., 1982, A&A, 115, 90
- Johnson, M. H., & Lippmann, B. A., 1949, Phys. Rev., 76, 828

- Mushtukov, A. A., Nagirner, D. I., & Poutanen, J. 2016, PhysRevD, 93, 105003
- Nagel, W. 1981, ApJ, 251, 288
- Nishimura, O. 2008, ApJ, 672, 1127
- Nobili, L., Turolla, R., & Zane, S. 2008a, MNRAS, 389, 989
- Nobili, L., Turolla, R., & Zane, S. 2008b, MNRAS, 386, 1527 (NTZ08b)
- Pavlov, G. G., Bezchastnov, V. G., Meszaros, P., & Alexander, S. G. 1991, ApJ, 380, 541
- Poutanen, J., Mushtukov, A. A., Suleimanov, V. F., et al. 2013, ApJ, 777, 115
- Schönherr, G., Wilms, J., Kretschmar, P. et al. 2007, A&A, 472, 353
- Schwarm, F.-W. 2017, PhD Thesis, Friedrich-Alexander Universität Sina, R. 1996, PhD Thesis, University of Maryland (unpublished)
- Sokolov, A. A., & Ternov, I.M. 1968, Radiation from Relativistic Electrons (American Institute of Physics, Melville, NY)
- Staubert, R., Trümper, J. E., Kendziorra, E. et al. 2019, A&A, 622, 61
- Trümper, J., Pietsch, W., Reppin, C., et al. 1977, Ann.N.Y.Acad.Sci, 302, 538
- Trümper, J., Pietsch, W., Reppin, C., et al. 1978, ApJ, 219, L105
- Ventura, J. 1979, Phys. Rev. D., 19, 1684
- Ventura, J., Nagel, W., & Meszaros, P. 1979, ApJ, 233, L125

Appendix A: Approximations resulting from the Harding & Daugherty (1991) expressions

We start from eq. (11) of Harding & Daugherty (1991) that has been derived in the electron's rest frame, considering that the electron initially occupies the ground state. In a unit system where $\hbar = c = m_e = 1$, this equation can be written as follows

$$\frac{d\sigma_{ss'}^{0,l}}{d\Omega'} = \frac{3\sigma_T \omega'}{4 \omega} \frac{\exp(-(\omega^2 \sin^2 \theta + \omega'^2 \sin^2 \theta')/2B)}{1 + \omega - \omega' - (\omega \cos \theta - \omega' \cos \theta') \cos \theta'} \times \left| \sum_{n=0}^{\infty} \sum_{i=1}^2 \left(F_{n,i}^{(1)} e^{i\Phi} + F_{n,i}^{(2)} e^{-i\Phi} \right) \right|^2, \quad (\text{A1})$$

where σ_T is the Thomson cross section, ω, ω' are the incident and scattered photon frequencies in units of $m_e c^2 / \hbar$, θ and θ' are the incident and scattered photon angles with respect to the magnetic field direction, B is the magnetic field strength \mathcal{B} (in units of \mathcal{B}_{cr}), Φ is proportional to $\sin(\phi - \phi')$, ϕ and ϕ' are the azimuthal angles of the incident and the scattered photon, respectively. The terms $F_{n,i}^{(1)}, F_{n,i}^{(2)}$ are complex functions of $\theta, \theta', \omega, \omega', B, \phi, \phi', s, s'$ and can be found in the Appendix of Harding & Daugherty (1991), where the upper indices 1, 2 are referred to the 1st and 2nd Feynman diagram. Furthermore, s and s' stand for the incident and scattered photon's polarization mode and l is the final electron's Landau state. Note that, the infinite sum in eq. (A1) is carried out over intermediate Landau states with principal quantum number n , whereas the sum over $i = 1, 2$ is for the possible electron spin orientations (spin-up, spin-down) in the intermediate state.

Equation (A1) is quite general, but this generality is not needed in most cases. Specifically, for resonant scattering of photons with energy $E \lesssim m_e c^2$ in a magnetic field smaller than or comparable to the critical one $\mathcal{B}_{cr} = m_e^2 c^3 / e \hbar$, Nobili, Turolla, & Zane (2008b, hereafter NTZ08b) pointed out that, for such magnetic fields, the probability of exciting Landau levels above the second ($n = 2$) is very small, thus the infinite sum over n in eq. (A1) becomes finite ($n \leq 2$).

Moreover, for photon energies $E \ll m_e c^2$, and magnetic fields $\mathcal{B} \ll \mathcal{B}_{cr}$, that we are interested in, the cross section expressions can be simplified even more, keeping only the term $n = 1$ in the sum over all the possible intermediate states and setting $l = 0$ for the final electron Landau state. Besides that, as NTZ08b stated, the $F_{n=1,i}^{(1)}$ terms exhibit a divergent behavior near resonant frequency (see their eqs. 7 and 8), while the terms $F_{n=1,i}^{(2)}$ remain instead finite. Given that, and as long as we are interested in resonant scattering (i.e. photon frequency near the resonant one), the above arguments lead us to a major simplification.

Neglecting all the non-resonant terms and the contributions of ($n \neq 1$) in eq. (A1), we deduce the following expression

$$\frac{d\sigma_{ss'}^{0,l=0}}{d\Omega'} = \frac{3\sigma_T \omega'}{4 \omega} \frac{\exp(-(\omega^2 \sin^2 \theta + \omega'^2 \sin^2 \theta')/2B)}{1 + \omega - \omega' - (\omega \cos \theta - \omega' \cos \theta') \cos \theta'} \times \left| F_{1,1}^{(1)} + F_{1,2}^{(1)} \right|^2. \quad (\text{A2})$$

NTZ08b have managed to write the above equation in a simpler way, obtaining compact expressions for the $F_{1,i}^{(1)}$

terms. Specifically, using eq. (14) of NTZ08b in eq. (10) of NTZ08b one gets

$$\frac{d\sigma_{ss'}}{d\Omega'} = \frac{3\sigma_T}{16\pi} \frac{\epsilon'}{\epsilon} \frac{(2 + \epsilon - \epsilon') \exp\left(-\frac{\epsilon^2 \sin^2 \theta + \epsilon'^2 \sin^2 \theta'}{2B}\right)}{1 + \epsilon - \epsilon' - (\epsilon \cos \theta - \epsilon' \cos \theta') \cos \theta'}$$

$$\times \left(\frac{1 + E_1}{2E_1}\right)^2 \left| \frac{T_+^{s \rightarrow s'}}{1 + \epsilon - E_1 + i\Gamma_+/2} + \frac{T_-^{s \rightarrow s'}}{1 + \epsilon - E_1 + i\Gamma_-/2} \right|^2, \quad (\text{A3})$$

where, for convenience, we retain the notation of NTZ08b, but for simplicity we drop the indices referring to $n = 1$ and $l = 0$. So, ϵ, ϵ' are the incident and scattered photon energies in units of $m_e c^2$, θ and θ' are the incident and scattered photon angles with respect to the magnetic field direction, B is the magnetic field strength \mathcal{B} (in units of \mathcal{B}_{cr}) and Γ_+, Γ_- are the relativistic decay rates corresponding to the $n=1$ intermediate state and are given by Herold, Ruder, & Wunner (1982, see also Harding & Daugherty 1991; Pavlov et al. 1991; Baring et al. 2005; NTZ08b), where the index "+" stands for the electron in the intermediate state with spin-up whereas the index "-" stands for spin-down. In addition, s and s' refer to the incident and scattered photon polarization modes, and the explicit expressions for the $T_+^{s \rightarrow s'}, T_-^{s \rightarrow s'}$ terms are given in the Appendix of NTZ08b for $n = 1$ and $l = 0$.

We remark that we do not use the relativistic polarization-dependent resonant Compton differential cross section expressions of NTZ08b, because, for their purposes, they substituted all the Lorentz profiles with a δ -function, and as a result the information about the exact shape of the different line profiles is lost.

The energy E_1 is the electron intermediate state and, in units of $m_e c^2$, it is given by eq. (12) of NTZ08b (see also eq. 4 of Harding & Daugherty 1991).

$$E_1 = \sqrt{1 + \epsilon^2 \cos^2 \theta + 2B}. \quad (\text{A4})$$

The energy ϵ' of the photon after scattering, in units of $m_e c^2$, is given by eq. (6) of NTZ08b (see also eq. 12 of Harding & Daugherty 1991)

$$\epsilon' = \frac{\epsilon^2 \sin^2 \theta + 2\epsilon}{1 + \epsilon(1 - \cos \theta \cos \theta') + \sqrt{f_1(\epsilon, \theta, \theta') + f_2(\epsilon, \theta, \theta')}}}, \quad (\text{A5a})$$

where

$$f_1(\epsilon, \theta, \theta') = 1 + 2\epsilon \cos \theta' (\cos \theta' - \cos \theta), \quad (\text{A5b})$$

and

$$f_2(\epsilon, \theta, \theta') = \epsilon^2 (\cos \theta - \cos \theta')^2. \quad (\text{A5c})$$

After a lengthy but straightforward calculation, and a trivial integration over the angle ϕ' , one can write eq. (A3) in the following way

$$\frac{d\sigma_{ss'}}{d \cos \theta'} = \frac{3\pi\sigma_T}{16} \frac{(1 + E_1)^2}{E_1 \sqrt{1 + 2B \sin^2 \theta}} \frac{\epsilon'}{\epsilon} A$$

$$\times \left[\frac{(T_+^{s \rightarrow s'})^2}{\Gamma_+} \mathcal{L}_+ + \frac{(T_-^{s \rightarrow s'})^2}{\Gamma_-} \mathcal{L}_- + 2 \frac{T_+^{s \rightarrow s'} T_-^{s \rightarrow s'}}{\Gamma_{mix}} \frac{\mathcal{L}_+ \mathcal{L}_-}{\mathcal{L}_{mix}} \right], \quad (\text{A6})$$

where the effective decay rates Γ_{\pm}^e , which result from the change in the Lorentz profiles argument (see NTZ08b), must be used in the Lorentz profiles (see eqs. A8-A10)

$$\Gamma_{\pm}^e = \frac{E_1(\epsilon_r)}{\sqrt{1 + 2B \sin^2 \theta}} \Gamma_{\pm} \quad (\text{A7a})$$

and we have defined the following function

$$A = \frac{(2 + \epsilon - \epsilon') \exp\left(-\frac{\epsilon^2 \sin^2 \theta + \epsilon'^2 \sin^2 \theta'}{2B}\right)}{1 + \epsilon - \epsilon' - (\epsilon \cos \theta - \epsilon' \cos \theta') \cos \theta'}. \quad (\text{A7b})$$

The quantities $\mathcal{L}_+(\epsilon, \epsilon_r)$, $\mathcal{L}_-(\epsilon, \epsilon_r)$ & $\mathcal{L}_{mix}(\epsilon, \epsilon_r)$ are the dimensionless Lorentz profiles and are given by

$$\mathcal{L}_+(\epsilon, \epsilon_r) = \frac{\Gamma_+^e/2\pi}{(\epsilon - \epsilon_r)^2 + (\Gamma_+^e/2)^2}, \quad (\text{A8})$$

$$\mathcal{L}_-(\epsilon, \epsilon_r) = \frac{\Gamma_-^e/2\pi}{(\epsilon - \epsilon_r)^2 + (\Gamma_-^e/2)^2}, \quad (\text{A9})$$

$$\mathcal{L}_{mix}(\epsilon, \epsilon_r) = \frac{\Gamma_{mix}^e/2\pi}{(\epsilon - \epsilon_r)^2 + (\Gamma_{mix}^e/2)^2}, \quad (\text{A10})$$

where Γ_{mix}^e is calculated by

$$\Gamma_{mix}^e = \frac{E_1(\epsilon_r)}{\sqrt{1 + 2B \sin^2 \theta}} \Gamma_{mix}, \quad (\text{A11a})$$

with

$$\Gamma_{mix} = \sqrt{\Gamma_+ \Gamma_-}, \quad (\text{A11b})$$

and ϵ_r is the resonant energy in units of $m_e c^2$. It is given by eq. (8) of NTZ08b (see also eq. 5 of Harding & Daugherty 1991)

$$\epsilon_r = \epsilon_1 = \frac{2B}{1 + \sqrt{1 + 2B \sin^2 \theta}}. \quad (\text{A12})$$

Having obtained the fully relativistic cross sections we proceed to the derivation of eqs. (4a)-(4d).

Expansion up to first order in the small parameters ϵ, ϵ' , and B yields

$$\frac{\epsilon'}{\epsilon} \approx 1 - \frac{\epsilon}{2} (\cos \theta - \cos \theta')^2, \quad (\text{A13})$$

$$\frac{(1 + E_1)^2}{E_1 \sqrt{1 + 2B \sin^2 \theta}} \frac{\epsilon'}{\epsilon} A \approx 8 \left[1 - B (2 \sin^2 \theta + (\cos \theta - \cos \theta')^2) \right]. \quad (\text{A14})$$

To lowest order, Γ_+, Γ_- are given in Herold, Ruder, & Wunner (1982) (see also eqs. 15, 16 of Harding & Daugherty 1991 and eq. 31 of NTZ08b)

$$\Gamma_+ \approx 2\alpha B^3/3, \quad (\text{A15a})$$

$$\Gamma_- \approx 4\alpha B^2/3, \quad (\text{A15b})$$

and substituting the above expressions into eq. (A11b) we get

$$\Gamma_{mix} \approx \frac{4}{3} \alpha B^2 \sqrt{B/2}, \quad (\text{A15c})$$

where α is the fine structure constant. For a discussion regarding the cyclotron line widths see our Appendix C.

Note that the classical cross sections (1) and the expressions (4) are proportional to $r_0 c$, while the quantum-mechanical ones are proportional to σ_T . This means that

the Lorentz profiles with variable the photon frequency (i.e. $L_+(\omega, \omega_r)$, $L_-(\omega, \omega_r)$ & $L_{mix}(\omega, \omega_r)$) have dimensions of time and their relation with the dimensionless ones (i.e. $\mathcal{L}_+(\epsilon, \epsilon_r)$, $\mathcal{L}_-(\epsilon, \epsilon_r)$ & $\mathcal{L}_{mix}(\epsilon, \epsilon_r)$) are (see Appendix C)

$$\mathcal{L}_+(\epsilon, \epsilon_r) \approx \frac{m_e c^2}{\hbar} L_+(\omega, \omega_r), \quad (A16a)$$

$$\mathcal{L}_-(\epsilon, \epsilon_r) \approx \frac{m_e c^2}{\hbar} L_-(\omega, \omega_r), \quad (A16b)$$

$$\mathcal{L}_{mix}(\epsilon, \epsilon_r) \approx \frac{m_e c^2}{\hbar} L_{mix}(\omega, \omega_r), \quad (A16c)$$

where the Lorentz profiles with argument the photon frequency are given by

$$L_+(\omega, \omega_r) = \frac{\Gamma'_+/2\pi}{(\omega - \omega_r)^2 + (\Gamma'_+/2)^2}, \quad (A17a)$$

$$L_-(\omega, \omega_r) = \frac{\Gamma'_-/2\pi}{(\omega - \omega_r)^2 + (\Gamma'_-/2)^2}, \quad (A17b)$$

$$L_{mix}(\omega, \omega_r) = \frac{\Gamma'_{mix}/2\pi}{(\omega - \omega_r)^2 + (\Gamma'_{mix}/2)^2}, \quad (A17c)$$

and

$$\Gamma'_+ = \frac{m_e c^2}{\hbar} \Gamma_+, \quad (A18a)$$

$$\Gamma'_- = \frac{m_e c^2}{\hbar} \Gamma_- \approx \Gamma = 4e^2 \omega_c^2 / (3m_e c^3), \quad (A18b)$$

$$\Gamma'_{mix} = \frac{m_e c^2}{\hbar} \Gamma_{mix}. \quad (A18c)$$

Using the above, one finds that eq. (A6) is approximated by the following one

$$\begin{aligned} \frac{d\sigma_{ss'}}{d\cos\theta'} &\approx \frac{3\pi\sigma_T m_e c^2}{2\hbar} W(B, \theta, \theta') \\ &\times \left[\frac{(T_+^{s \rightarrow s'})^2}{\Gamma_+} L_+ + \frac{(T_-^{s \rightarrow s'})^2}{\Gamma_-} L_- + 2 \frac{T_+^{s \rightarrow s'} T_-^{s \rightarrow s'}}{\Gamma_{mix}} \frac{L_+ L_-}{L_{mix}} \right], \\ &= 2\pi \frac{3\pi r_o c}{8} \left(\frac{16\alpha}{3} \right) W(B, \theta, \theta') \\ &\times \left[\frac{(T_+^{s \rightarrow s'})^2}{\Gamma_+} L_+ + \frac{(T_-^{s \rightarrow s'})^2}{\Gamma_-} L_- + 2 \frac{T_+^{s \rightarrow s'} T_-^{s \rightarrow s'}}{\Gamma_{mix}} \frac{L_+ L_-}{L_{mix}} \right], \end{aligned} \quad (A19)$$

where

$$W(B, \theta, \theta') = 1 - B (2 \sin^2 \theta + (\cos \theta - \cos \theta')^2), \quad (A20)$$

and we have used that

$$\epsilon \approx \epsilon_r \approx B. \quad (A21)$$

The expressions for $T_+^{s \rightarrow s'}$ and $T_-^{s \rightarrow s'}$ have strong polarization dependence and, as we mentioned earlier, are given in the Appendix of NTZ08b. In order to obtain equations (4), we will work separately for each pair s, s' .

A.1. Transition $1 \rightarrow 1$

By expanding the terms $T_+^{1 \rightarrow 1}$, $T_-^{1 \rightarrow 1}$ in the small parameters ϵ, ϵ' , and B , and employing eqs. (A15) and (A21), one obtains the following approximations

$$\frac{(T_+^{1 \rightarrow 1})^2}{\Gamma_+} \approx \frac{3}{16\alpha} \left(\frac{B}{2} \right), \quad (A22a)$$

$$\begin{aligned} \frac{(T_-^{1 \rightarrow 1})^2}{\Gamma_-} &\approx \frac{3}{16\alpha} \cos^2 \theta \cos^2 \theta' \\ &\times \left[1 - B \left(2 + \sin^2 \theta + \frac{2 \sin^2 \theta' \cos \theta}{\cos \theta'} - \sin^2 \theta' \right) \right], \end{aligned} \quad (A22b)$$

$$\frac{2T_+^{1 \rightarrow 1} T_-^{1 \rightarrow 1}}{\Gamma_{mix}} \approx \frac{3}{16\alpha} \sqrt{2B} \cos \theta \cos \theta'. \quad (A22c)$$

Equations (A22), along with (A19), lead us to derive the following approximation for $d\sigma_{11}/d\cos\theta'$

$$\begin{aligned} \frac{d\sigma_{11}}{d\cos\theta'} &\approx 2\pi \frac{3\pi r_o c}{8} \left[g^{1 \rightarrow 1} \cdot L_- + h^{1 \rightarrow 1} \cdot L_+ \right. \\ &\left. + \sqrt{2B} \cos \theta \cos \theta' \frac{L_- \cdot L_+}{L_{mix}} \right], \end{aligned} \quad (A23a)$$

where

$$\begin{aligned} g^{1 \rightarrow 1}(\theta, \theta', B) &= \cos^2 \theta \cos^2 \theta' \left[1 - B \left(3 \sin^2 \theta - \sin^2 \theta' \right. \right. \\ &\left. \left. + (\cos \theta - \cos \theta')^2 + 2 + 2 \sin^2 \theta' \frac{\cos \theta}{\cos \theta'} \right) \right], \end{aligned} \quad (A23b)$$

and

$$h^{1 \rightarrow 1}(B) = \frac{B}{2}. \quad (A23c)$$

A.2. Transition $1 \rightarrow 2$

We apply the same methodology to all the other cases. Hence, by expanding the terms $T_+^{1 \rightarrow 2}$, $T_-^{1 \rightarrow 2}$ in the small parameters ϵ, ϵ' , and B , and using eqs. (A15) and (A21), one finds the following approximations

$$\frac{(T_+^{1 \rightarrow 2})^2}{\Gamma_+} \approx \frac{3}{16\alpha} \left(\frac{B}{2} \cos^2 \theta' \right), \quad (A24a)$$

$$\frac{(T_-^{1 \rightarrow 2})^2}{\Gamma_-} \approx \frac{3}{16\alpha} \cos^2 \theta [1 - B (2 + \sin^2 \theta)], \quad (A24b)$$

$$\frac{2T_+^{1 \rightarrow 2} T_-^{1 \rightarrow 2}}{\Gamma_{mix}} \approx \frac{3}{16\alpha} \sqrt{2B} \cos \theta \cos \theta'. \quad (A24c)$$

Then, by substituting eqs. (A24) into eq. (A19) one gets the following approximation

$$\begin{aligned} \frac{d\sigma_{12}}{d\cos\theta'} &\approx 2\pi \frac{3\pi r_o c}{8} \left[g^{1 \rightarrow 2} \cdot L_- + h^{1 \rightarrow 2} \cdot L_+ \right. \\ &\left. + \sqrt{2B} \cos \theta \cos \theta' \frac{L_- \cdot L_+}{L_{mix}} \right], \end{aligned} \quad (A25a)$$

where

$$g^{1 \rightarrow 2}(\theta, \theta', B) = \cos^2 \theta \left[1 - B \left(3 \sin^2 \theta + 2 + (\cos \theta - \cos \theta')^2 \right) \right], \quad (A25b)$$

and

$$h^{1 \rightarrow 2}(\theta', B) = \frac{B}{2} \cos^2 \theta'. \quad (A25c)$$

A.3. Transition $2 \rightarrow 1$

Similarly, by expanding the terms $T_+^{2 \rightarrow 1}$, $T_-^{2 \rightarrow 1}$ in the small parameters ϵ , ϵ' , and B , and taking into account eqs. (A15) and (A21), one deduces the following approximations

$$\frac{(T_+^{2 \rightarrow 1})^2}{\Gamma_+} \approx \frac{3}{16\alpha} \left(\frac{B}{2} \cos^2 \theta \right), \quad (A26a)$$

$$\frac{(T_-^{2 \rightarrow 1})^2}{\Gamma_-} \approx \frac{3}{16\alpha} \cos^2 \theta' \times \left[1 - B \left(2 - \sin^2 \theta' + 2 \sin^2 \theta' \frac{\cos \theta}{\cos \theta'} \right) \right], \quad (A26b)$$

$$\frac{2T_+^{2 \rightarrow 1}T_-^{2 \rightarrow 1}}{\Gamma_{mix}} \approx \frac{3}{16\alpha} \sqrt{2B} \cos \theta \cos \theta'. \quad (A26c)$$

Using eqs. (A26) and (A19), one finds

$$\frac{d\sigma_{21}}{d \cos \theta'} \approx 2\pi \frac{3\pi r_o c}{8} \left[g^{2 \rightarrow 1} \cdot L_- + h^{2 \rightarrow 1} \cdot L_+ + \sqrt{2B} \cos \theta \cos \theta' \frac{L_- \cdot L_+}{L_{mix}} \right], \quad (A27a)$$

where

$$g^{2 \rightarrow 1}(\theta, \theta', B) = \cos^2 \theta' \left[1 - B \left(2 \sin^2 \theta + (\cos \theta - \cos \theta')^2 + 2 - \sin^2 \theta' + 2 \sin^2 \theta' \frac{\cos \theta}{\cos \theta'} \right) \right], \quad (A27b)$$

and

$$h^{2 \rightarrow 1}(\theta, B) = \frac{B}{2} \cos^2 \theta. \quad (A27c)$$

A.4. Transition $2 \rightarrow 2$

Following the same procedure as above, for the terms $T_+^{2 \rightarrow 2}$, $T_-^{2 \rightarrow 2}$ and employing eqs. (A15) and (A21), one derives that

$$\frac{(T_+^{2 \rightarrow 2})^2}{\Gamma_+} \approx \frac{3}{16\alpha} \left(\frac{B}{2} \cos^2 \theta \cos^2 \theta' \right), \quad (A28a)$$

$$\frac{(T_-^{2 \rightarrow 2})^2}{\Gamma_-} \approx \frac{3}{16\alpha} (1 - 2B), \quad (A28b)$$

$$\frac{2T_+^{2 \rightarrow 2}T_-^{2 \rightarrow 2}}{\Gamma_{mix}} \approx \frac{3}{16\alpha} \sqrt{2B} \cos \theta \cos \theta'. \quad (A28c)$$

Thus, the substitution of eqs. (A28) into (A19), yields

$$\frac{d\sigma_{22}}{d \cos \theta'} \approx 2\pi \frac{3\pi r_o c}{8} \left[g^{2 \rightarrow 2} \cdot L_- + h^{2 \rightarrow 2} \cdot L_+ + \sqrt{2B} \cos \theta \cos \theta' \frac{L_- \cdot L_+}{L_{mix}} \right], \quad (A29a)$$

where

$$g^{2 \rightarrow 2}(\theta, \theta', B) = 1 - B [2 \sin^2 \theta + (\cos \theta - \cos \theta')^2 + 2], \quad (A29b)$$

and

$$h^{2 \rightarrow 2}(\theta, \theta', B) = \frac{B}{2} \cos^2 \theta \cos^2 \theta'. \quad (A29c)$$

Appendix B: Approximations resulting from the Sina (1996) expressions

We start from eq. (3.25) of Sina (1996), written in the electron's rest frame (ground state), considering a unit system where $\hbar = m_e = c = 1$, (i.e. energy is measured in $m_e c^2$, frequency is measured in $m_e c^2 / \hbar$ and the magnetic field strength \mathcal{B} is measured in $\mathcal{B}_{cr} = e^{-1}$) and neglect terms that are related to the 2nd Feynman diagram, as well as the terms that the intermediate electron Landau state has a principal quantum number $n \neq 1$ (i.e. keeping only the terms that exhibit a divergence near resonant frequency with $n = 1$, as we did in Appendix A). So, the infinite sum over n for all possible intermediate states collapses to the following

$$\frac{d\sigma_{ss'}}{d\Omega_f} = \frac{\alpha^2}{1 - \beta_f \cos \theta_f} \frac{\omega_f}{\omega_i} |Z_{c1}(n=1)|^2, \quad (B1a)$$

where $Z_{c1}(n=1)$ is given by eq. (3.15) of Sina (1996) and is a sum over the possible electron spin orientations s_n in the intermediate state (for spin-up $s_n = +1$ whereas for spin-down $s_n = -1$)

$$Z_{c1}(n=1) = \sum_{s_n} \frac{D^{f,n=1,s_f,s_n}(k_f) H^{n=1,i,s_n,s_i}(k_i)}{\omega_i + E_i - E_{n=1,1} + i\Gamma_{s_n}^{n=1}/2}. \quad (B1b)$$

We retain the notation of Sina (1996), so ω_i is the incident photon frequency, E_i is the electron's energy before scattering, θ_i, θ_f are the incident and scattered photon angles with respect to the magnetic field direction, the indices i and f stand for the initial and final electron Landau states (in our case they are equal to 0, i.e. ground state), the s_i and s_f are the initial and final electron's spin orientations and are equal to -1 (since only spin-down is allowed in the ground state), and k_i, k_f are the incident and scattered electron wavenumbers, respectively. Furthermore, $E_{n=1,1}$ (E_1 , hereafter) is the electron's energy in the intermediate state with $n = 1$ and is given by eq. (3.3) of Sina (1996) (see also eq. 3.1 of Schwarm 2017)

$$E_1 \equiv E_{n=1,1} = \sqrt{1 + \omega_i^2 \cos^2 \theta_i + 2B}, \quad (B2)$$

where a misprint has been corrected and we have substituted eq. (3.4) of Sina (1996) into eq. (3.3) of Sina (1996) and took into account that the initial electron momentum p_i is equal to zero, since we work in the electron's rest frame. Moreover, β_f can be written as p_f/E_f (see eq. B18

of Gonthier et al. 2014), where E_f and p_f are the final electron energy and parallel component of momentum (with respect to the magnetic field direction) and are calculated by imposing the conservation of energy and by eq. (3.29) of Sina (1996). Thus

$$E_f = 1 + \omega_i - \omega_f, \quad (B3a)$$

and

$$p_f = \omega_i \cos \theta_i - \omega_f \cos \theta_f. \quad (B3b)$$

Note that ω_f is the scattered photon frequency and is given by eq. (3.28) of Sina (1996), although it is actually our eq. (A5) written in a different form, so we do not present it here and $\Gamma_{s_n=+1}^{n=1}$, $\Gamma_{s_n=-1}^{n=1}$ (Γ_+ , Γ_- , hereafter) are the relativistic decay widths for the electron in the intermediate state with spin-up and spin-down, respectively, and are given by Herold, Ruder, & Wunner (1982). Fig. 3.4 of Schwarm (2017) verifies that the decay widths of Sina (1996) are in full agreement with the ones of Herold, Ruder, & Wunner (1982) that we have used in Appendix A. This is reasonable and absolutely predictable, since both works have employed electron wavefunctions of Sokolov & Ternov (1968).

Substituting the above into eqs. (B1) and using that the initial electron energy E_1 is equal to 1 and $\alpha^2 = 3\sigma_T/8\pi$ in this system of units, we obtain

$$\begin{aligned} \frac{d\sigma_{ss'}}{d\Omega_f} &= \frac{3\sigma_T}{8\pi} \frac{1 + \omega_i - \omega_f}{1 + \omega_i - \omega_f - (\omega_i \cos \theta_i - \omega_f \cos \theta_f) \cos \theta_f} \\ &\times \frac{\omega_f}{\omega_i} \left| \frac{D^{f=0,n=1,s_f=-1,s_n=+1}(k_f) H^{n=1,i=0,s_n=+1,s_i=-1}(k_i)}{1 + \omega_i - E_1 + i\Gamma_+/2} \right. \\ &\left. + \frac{D^{f=0,n=1,s_f=-1,s_n=-1}(k_f) H^{n=1,i=0,s_n=-1,s_i=-1}(k_i)}{1 + \omega_i - E_1 + i\Gamma_-/2} \right|^2, \quad (B4) \end{aligned}$$

where the complex functions $D^{f,n,s_f,s_n}(k_f)$ and $H^{n,i,s_n,s_i}(k_i)$ have strong polarization dependence, since they depend on the polarization modes of the incident and scattered photons, and are given in Appendix D of Sina (1996). Specifically, the $D^{f,n,s_f,s_n}(k_f)$ terms exclusively depend on the final photon polarization mode and are calculated by eqs. (D.61), (D.66) of Sina (1996)

$$\begin{aligned} D_{\perp}^{f=0,n=1,s_f=-1,s_n}(k_f) &= \\ &i \left[(C_{1,f=0}C_{4,n=1} + C_{3,f=0}C_{2,n=1})\Lambda_{-1,1}(k_f) - \right. \\ &\left. (C_{2,f=0}C_{3,n=1} + C_{4,f=0}C_{1,n=1})\Lambda_{0,0}(k_f) \right], \quad (B5a) \end{aligned}$$

$$\begin{aligned} D_{\parallel}^{f=0,n=1,s_f=-1,s_n}(k_f) &= \\ &\cos \theta_f \left[(C_{1,f=0}C_{4,n=1} + C_{3,f=0}C_{2,n=1})\Lambda_{-1,1}(k_f) + \right. \\ &\left. (C_{2,f=0}C_{3,n=1} + C_{4,f=0}C_{1,n=1})\Lambda_{0,0}(k_f) \right] - \\ &\sin \theta_f \left[(C_{1,f=0}C_{3,n=1} + C_{3,f=0}C_{1,n=1})\Lambda_{-1,0}(k_f) - \right. \\ &\left. (C_{2,f=0}C_{4,n=1} + C_{4,f=0}C_{2,n=1})\Lambda_{0,1}(k_f) \right], \quad (B5b) \end{aligned}$$

while the terms $H^{n,i,s_n,s_i}(k_i)$ exclusively depend on the initial photon polarization mode and are given by eqs. (D.60), (D.65) of Sina (1996)

$$\begin{aligned} H_{\perp}^{n=1,i=0,s_n,s_i=-1}(k_i) &= \\ &i \left[(C_{1,n=1}C_{4,i=0} + C_{3,n=1}C_{2,i=0})\Lambda_{0,0}(k_i) - \right. \\ &\left. (C_{2,n=1}C_{3,i=0} + C_{4,n=1}C_{1,i=0})\Lambda_{-1,1}(k_i) \right], \quad (B6a) \end{aligned}$$

$$\begin{aligned} H_{\parallel}^{n=1,i=0,s_n,s_i=-1}(k_i) &= \\ &\cos \theta_i \left[(C_{1,n=1}C_{4,i=0} + C_{3,n=1}C_{2,i=0})\Lambda_{0,0}(k_i) + \right. \\ &\left. (C_{2,n=1}C_{3,i=0} + C_{4,n=1}C_{1,i=0})\Lambda_{-1,1}(k_i) \right] - \\ &\sin \theta_i \left[(C_{1,n=1}C_{3,i=0} + C_{3,n=1}C_{1,i=0})\Lambda_{-1,0}(k_i) - \right. \\ &\left. (C_{2,n=1}C_{4,i=0} + C_{4,n=1}C_{2,i=0})\Lambda_{0,1}(k_i) \right], \quad (B6b) \end{aligned}$$

where the lower index “ \parallel ” stands for the ordinary polarization mode whereas the lower index “ \perp ” stands for the extraordinary polarization mode. Moreover the quantities C_k with $k=1,2,3,4$, are the wavefunction coefficients of Sokolov & Ternov (1968) and are given by eqs. (B61)-(B65) of Sina (1996), whereas the $\Lambda_{i,j}$ functions are proportional to Laguerre polynomials and are given in Appendix D of Sina (1996). Note that, one can also obtain all of the above using Appendix B of Gonthier et al. (2014).

After a lengthy, but straightforward calculation, we can write eq. (B4) in the following form

$$\begin{aligned} \frac{d\sigma_{ss'}}{d\cos\theta_f} &= \frac{3\pi\sigma_T}{2} \frac{E_1}{\sqrt{1+2B\sin^2\theta_i}} \frac{\omega_f}{\omega_i} \mathcal{A} \\ &\times \left[\frac{\mathcal{T}_+^{s \rightarrow s'}}{\Gamma_+} \mathcal{L}_+ + \frac{\mathcal{T}_-^{s \rightarrow s'}}{\Gamma_-} \mathcal{L}_- + 2 \frac{\mathcal{T}_{mix}^{s \rightarrow s'}}{\Gamma_{mix}} \frac{\mathcal{L}_+ \mathcal{L}_-}{\mathcal{L}_{mix}} \right], \quad (B7a) \end{aligned}$$

where we have done a trivial integration over the scattered photon azimuthal angle ϕ_f . Also, for simplicity, we have defined the following quantities

$$\mathcal{A} = \frac{(1 + \omega_i - \omega_f) \exp(-(\omega_i^2 \sin^2 \theta_i + \omega_f^2 \sin^2 \theta_f)/2B)}{1 + \omega_i - \omega_f - (\omega_i \cos \theta_i - \omega_f \cos \theta_f) \cos \theta_f}, \quad (B7b)$$

$$\begin{aligned} \mathcal{T}_+^{s \rightarrow s'} &= \exp((\omega_i^2 \sin^2 \theta_i + \omega_f^2 \sin^2 \theta_f)/2B) \\ &\times \left| D_{s'}^{f=0,n=1,s_f=-1,s_n=+1} H_s^{n=1,i=0,s_n=+1,s_i=-1} \right|^2, \quad (B7c) \end{aligned}$$

$$\begin{aligned} \mathcal{T}_-^{s \rightarrow s'} &= \exp((\omega_i^2 \sin^2 \theta_i + \omega_f^2 \sin^2 \theta_f)/2B) \\ &\times \left| D_{s'}^{f=0,n=1,s_f=-1,s_n=-1} H_s^{n=1,i=0,s_n=-1,s_i=-1} \right|^2, \quad (B7d) \end{aligned}$$

$$\begin{aligned}
2\mathcal{T}_{mix}^{s \rightarrow s'} &= \exp((\omega_i^2 \sin^2 \theta_i + \omega_f^2 \sin^2 \theta_f)/2B) \\
&\times \left[\left((D_{s'}^{f=0, n=1, s_f=-1, s_n=+1} H_s^{n=1, i=0, s_n=+1, s_i=-1})^* \right. \right. \\
&\quad \times \left. \left. D_{s'}^{f=0, n=1, s_f=-1, s_n=-1} H_s^{n=1, i=0, s_n=-1, s_i=-1} \right) + \right. \\
&\quad \left(D_{s'}^{f=0, n=1, s_f=-1, s_n=+1} H_s^{n=1, i=0, s_n=+1, s_i=-1} \right. \\
&\quad \left. \times \left. (D_{s'}^{f=0, n=1, s_f=-1, s_n=-1} H_s^{n=1, i=0, s_n=-1, s_i=-1})^* \right) \right]. \tag{B7e}
\end{aligned}$$

Note that the dimensionless Lorentz profiles $\mathcal{L}_+(\omega_i, \omega_r)$, $\mathcal{L}_-(\omega_i, \omega_r)$, and $\mathcal{L}_{mix}(\omega_i, \omega_r)$ that are shown in eq. (B7a) are the same as the ones in Appendix A, since in this unit system the dimensionless photon frequencies ω_i, ω_f and the dimensionless resonant frequency, have the same values with the corresponding dimensionless energies and, as we mentioned earlier, the decay widths are identical to those shown in Appendix A (and so are the effective decay widths given by eqs. A7a, A11b). Furthermore, the dimensionless resonant frequency ω_r is given by eq. (5) of Harding & Daugherty (1991) and is actually the same as the dimensionless resonant energy (eq. A12) in Appendix A

$$\omega_r = \frac{2B}{1 + \sqrt{1 + 2B \sin^2 \theta_i}}. \tag{B8}$$

Having obtained eqs. (B7), we are able to proceed to the derivation of eqs. (5a)-(5d). Expansion up to first order in the small parameters ω_i, ω_f , and B yields

$$\frac{\omega_f}{\omega_i} \approx 1 - \frac{\omega_i}{2} (\cos \theta_i - \cos \theta_f)^2, \tag{B9}$$

$$\frac{\omega_f E_1 \cdot \mathcal{A}}{\omega_i \sqrt{1 + 2B \sin^2 \theta_i}} \approx 1 - B (\sin^2 \theta_i + \cos^2 \theta_f - 2 \cos \theta_i \cos \theta_f) \tag{B10}$$

$$\omega_i \approx \omega_r \approx B. \tag{B11}$$

Using the above, one finds that eq. (B7a) can be approximated by

$$\begin{aligned}
\frac{d\sigma_{ss'}}{d \cos \theta_f} &\approx \frac{3\pi\sigma_T}{2} \mathcal{W}(\theta_i, \theta_f, B) \\
&\times \left[\frac{\mathcal{T}_+^{s \rightarrow s'}}{\Gamma_+} \mathcal{L}_+ + \frac{\mathcal{T}_-^{s \rightarrow s'}}{\Gamma_-} \mathcal{L}_- + 2 \frac{\mathcal{T}_{mix}^{s \rightarrow s'}}{\Gamma_{mix}} \frac{\mathcal{L}_+ \mathcal{L}_-}{\mathcal{L}_{mix}} \right], \tag{B12}
\end{aligned}$$

and recalling the dimensions of each quantity by taking into account the procedure as well as the results of Appendix A, we obtain the following approximation

$$\begin{aligned}
\frac{d\sigma_{ss'}}{d \cos \theta_f} &\approx 2\pi \frac{3\pi r_o c}{8} \left(\frac{16\alpha}{3} \right) \mathcal{W}(\theta_i, \theta_f, B) \\
&\times \left[\frac{\mathcal{T}_+^{s \rightarrow s'}}{\Gamma_+} L_+ + \frac{\mathcal{T}_-^{s \rightarrow s'}}{\Gamma_-} L_- + 2 \frac{\mathcal{T}_{mix}^{s \rightarrow s'}}{\Gamma_{mix}} \frac{L_+ L_-}{L_{mix}} \right], \tag{B13a}
\end{aligned}$$

where

$$\mathcal{W}(\theta_i, \theta_f, B) = 1 - B (\sin^2 \theta_i + \cos^2 \theta_f - 2 \cos \theta_i \cos \theta_f). \tag{B13b}$$

From now on, all the quantities have their physical dimensions and as a result the Lorentz profiles that are shown in eq. (B13a) have dimensions of time and are calculated by eqs. (A17), where, in the notation that we use in this Appendix, the arguments of $L_+(\omega_i, \omega_r)$, $L_-(\omega_i, \omega_r)$, and $L_{mix}(\omega_i, \omega_r)$ are ω_i and ω_r . As we said earlier, the terms $\mathcal{T}_+^{s \rightarrow s'}$, $\mathcal{T}_-^{s \rightarrow s'}$, and $\mathcal{T}_{mix}^{s \rightarrow s'}$ have strong polarization dependence and for this reason we are going to derive the approximations separately for each possible combination of the incident and scattered photon polarization modes.

B.1. Transition $1 \rightarrow 1$

By expanding the terms $\mathcal{T}_+^{1 \rightarrow 1}$, $\mathcal{T}_-^{1 \rightarrow 1}$, and $\mathcal{T}_{mix}^{1 \rightarrow 1}$ in the small parameters ω_i, ω_f , and B , and employing eqs. (A15) and (B11), one obtains the following approximations

$$\frac{\mathcal{T}_+^{1 \rightarrow 1}}{\Gamma_+} \approx \frac{3}{16\alpha} \left(\frac{B}{2} \right), \tag{B14a}$$

$$\begin{aligned}
\frac{\mathcal{T}_-^{1 \rightarrow 1}}{\Gamma_-} &\approx \frac{3}{16\alpha} \cos^2 \theta_i \cos^2 \theta_f \\
&\times \left[1 - B \left(\sin^2 \theta_i + \frac{2 \sin^2 \theta_f \cos \theta_i}{\cos \theta_f} - \sin^2 \theta_f \right) \right], \tag{B14b}
\end{aligned}$$

$$\frac{2\mathcal{T}_{mix}^{1 \rightarrow 1}}{\Gamma_{mix}} \approx \frac{3}{16\alpha} \sqrt{2B} \cos \theta_i \cos \theta_f. \tag{B14c}$$

Equations (B14) along with (B13) lead us to derive the following approximation for $d\sigma_{11}/d \cos \theta_f$

$$\begin{aligned}
\frac{d\sigma_{11}}{d \cos \theta_f} &\approx 2\pi \frac{3\pi r_o c}{8} \left[\mathcal{G}^{1 \rightarrow 1} \cdot L_- + h^{1 \rightarrow 1} \cdot L_+ \right. \\
&\quad \left. + \sqrt{2B} \cos \theta_i \cos \theta_f \frac{L_- \cdot L_+}{L_{mix}} \right], \tag{B15a}
\end{aligned}$$

where

$$\begin{aligned}
\mathcal{G}^{1 \rightarrow 1}(\theta_i, \theta_f, B) &= \cos^2 \theta_i \cos^2 \theta_f \left[1 - B \left(3 \sin^2 \theta_i - \sin^2 \theta_f \right. \right. \\
&\quad \left. \left. + (\cos \theta_i - \cos \theta_f)^2 - 1 + 2 \sin^2 \theta_f \frac{\cos \theta_i}{\cos \theta_f} \right) \right], \tag{B15b}
\end{aligned}$$

and

$$h^{1 \rightarrow 1}(B) = \frac{B}{2}. \tag{B15c}$$

B.2. Transition $1 \rightarrow 2$

We apply the same methodology to all the other cases. Hence, by expanding the terms $\mathcal{T}_+^{1 \rightarrow 2}$, $\mathcal{T}_-^{1 \rightarrow 2}$, and $\mathcal{T}_{mix}^{1 \rightarrow 2}$ in the small parameters ω_i, ω_f , and B , and employing eqs. (A15) and (B11), one finds the following approximations

$$\frac{\mathcal{T}_+^{1 \rightarrow 2}}{\Gamma_+} \approx \frac{3}{16\alpha} \left(\frac{B}{2} \cos^2 \theta_f \right), \tag{B16a}$$

$$\frac{\mathcal{T}_-^{1 \rightarrow 2}}{\Gamma_-} \approx \frac{3}{16\alpha} \cos^2 \theta_i (1 - B \sin^2 \theta_i), \tag{B16b}$$

$$\frac{2\mathcal{T}_{mix}^{1 \rightarrow 2}}{\Gamma_{mix}} \approx \frac{3}{16\alpha} \sqrt{2B} \cos \theta_i \cos \theta_f. \tag{B16c}$$

Then, by substituting eqs. (B16) into eq. (B13a) one gets the following approximation

$$\frac{d\sigma_{12}}{d\cos\theta_f} \approx 2\pi \frac{3\pi r_o c}{8} \left[\mathcal{G}^{1\rightarrow 2} \cdot L_- + h^{1\rightarrow 2} \cdot L_+ + \sqrt{2B} \cos\theta_i \cos\theta_f \frac{L_- \cdot L_+}{L_{mix}} \right], \quad (\text{B17a})$$

where

$$\mathcal{G}^{1\rightarrow 2}(\theta_i, \theta_f, B) = \cos^2\theta_i \left[1 - B \left(3\sin^2\theta_i - 1 + (\cos\theta_i - \cos\theta_f)^2 \right) \right], \quad (\text{B17b})$$

and

$$h^{1\rightarrow 2}(\theta_f, B) = \frac{B}{2} \cos^2\theta_f. \quad (\text{B17c})$$

B.3. Transition $2 \rightarrow 1$

Similarly, by expanding the terms $\mathcal{T}_+^{2\rightarrow 1}$, $\mathcal{T}_-^{2\rightarrow 1}$, and $\mathcal{T}_{mix}^{2\rightarrow 1}$ in the small parameters ω_i, ω_f , and B , and taking into account eqs. (A15) and (B11), one deduces the following approximations

$$\frac{\mathcal{T}_+^{2\rightarrow 1}}{\Gamma_+} \approx \frac{3}{16\alpha} \left(\frac{B}{2} \cos^2\theta_i \right), \quad (\text{B18a})$$

$$\frac{\mathcal{T}_-^{2\rightarrow 1}}{\Gamma_-} \approx \frac{3}{16\alpha} \cos^2\theta_f \times \left[1 - B \left(2\sin^2\theta_f \frac{\cos\theta_i}{\cos\theta_f} - \sin^2\theta_f \right) \right], \quad (\text{B18b})$$

$$\frac{2\mathcal{T}_{mix}^{2\rightarrow 1}}{\Gamma_{mix}} \approx \frac{3}{16\alpha} \sqrt{2B} \cos\theta_i \cos\theta_f. \quad (\text{B18c})$$

Using eqs. (B18) and (B13a), one finds

$$\frac{d\sigma_{21}}{d\cos\theta_f} \approx 2\pi \frac{3\pi r_o c}{8} \left[\mathcal{G}^{2\rightarrow 1} \cdot L_- + h^{2\rightarrow 1} \cdot L_+ + \sqrt{2B} \cos\theta_i \cos\theta_f \frac{L_- \cdot L_+}{L_{mix}} \right], \quad (\text{B19a})$$

where

$$\mathcal{G}^{2\rightarrow 1}(\theta_i, \theta_f, B) = \cos^2\theta_f \left[1 - B \left(2\sin^2\theta_i + (\cos\theta_i - \cos\theta_f)^2 - 1 - \sin^2\theta_f + 2\sin^2\theta_f \frac{\cos\theta_i}{\cos\theta_f} \right) \right], \quad (\text{B19b})$$

and

$$h^{2\rightarrow 1}(\theta_i, B) = \frac{B}{2} \cos^2\theta_i. \quad (\text{B19c})$$

B.4. Transition $2 \rightarrow 2$

Following the same procedure as above for the terms $\mathcal{T}_+^{2\rightarrow 2}$, $\mathcal{T}_-^{2\rightarrow 2}$, and $\mathcal{T}_{mix}^{2\rightarrow 2}$ and employing eqs. (A15) and (B11), one derives that

$$\frac{\mathcal{T}_+^{2\rightarrow 2}}{\Gamma_+} \approx \frac{3}{16\alpha} \left(\frac{B}{2} \cos^2\theta_i \cos^2\theta_f \right), \quad (\text{B20a})$$

$$\frac{\mathcal{T}_-^{2\rightarrow 2}}{\Gamma_-} \approx \frac{3}{16\alpha}, \quad (\text{B20b})$$

$$\frac{2\mathcal{T}_{mix}^{2\rightarrow 2}}{\Gamma_{mix}} \approx \frac{3}{16\alpha} \sqrt{2B} \cos\theta_i \cos\theta_f. \quad (\text{B20c})$$

Thus, the substitution of eqs. (B20) into (B13a), yields

$$\frac{d\sigma_{22}}{d\cos\theta_f} \approx 2\pi \frac{3\pi r_o c}{8} \left[\mathcal{G}^{2\rightarrow 2} \cdot L_- + h^{2\rightarrow 2} \cdot L_+ + \sqrt{2B} \cos\theta_i \cos\theta_f \frac{L_- \cdot L_+}{L_{mix}} \right], \quad (\text{B21a})$$

where

$$\mathcal{G}^{2\rightarrow 2}(\theta_i, \theta_f, B) = 1 - B [2\sin^2\theta_i + (\cos\theta_i - \cos\theta_f)^2 - 1], \quad (\text{B21b})$$

and

$$h^{2\rightarrow 2}(\theta_i, \theta_f, B) = \frac{B}{2} \cos^2\theta_i \cos^2\theta_f. \quad (\text{B21c})$$

Appendix C: Cyclotron line widths

The spin dependent relativistic cyclotron widths Γ_+ , Γ_- for the transitions from the 1st excited intermediate electron state to the fundamental $n = 0$ Landau state are given by eq. (17) of Herold et al. (1982) or/and by eq. (3) of Pavlov et al. (1991). So, we do not present the complete formulae here.

Known in the literature are the non-relativistic cyclotron line widths, which consist of the dominant terms and are valid for small magnetic fields ($\mathcal{B} \ll \mathcal{B}_{cr}$) (see Herold et al. 1982; NTZ08b).

$$\Gamma_+ \approx 2\alpha B^3/3, \quad (\text{C1a})$$

$$\Gamma_- \approx 4\alpha B^2/3. \quad (\text{C1b})$$

For users who would like to have more accuracy, we provide below next order corrections in B . These corrections have been derived from numerical fits to the relativistic transition rates of Herold et al. (1982).

$$\Gamma_+ \approx \frac{2}{3}\alpha B^3(1 - 2.9B), \quad (\text{C2a})$$

$$\Gamma_- \approx \frac{4}{3}\alpha B^2(1 - 2.7B). \quad (\text{C2b})$$

In Fig. 8 we display the relativistic decay rates of Herold (1982), along with the non-relativistic ones and the expressions C2, which have a first order correction in B .

Clearly the non-relativistic expressions given by eq. (C1) can be used in the Lorentz profiles (defined by eq. A17) in the case where $B \ll 1$

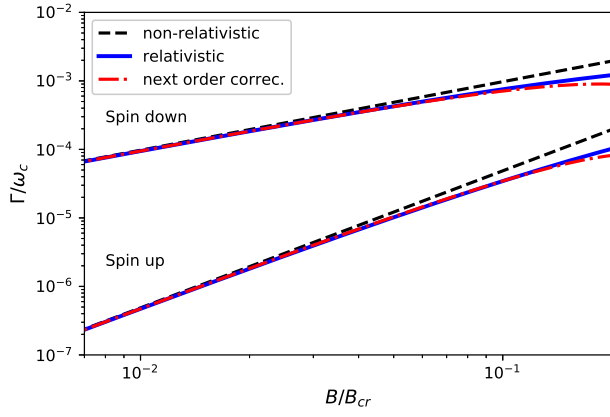


Fig. C.1. Comparison of the relativistic transition rates of Herold et al. (1982) (blue solid lines) with the non-relativistic ones (eq. A15) (black dashed lines) and with the expressions given by eq. (C2) (red dash-dotted lines). Spin up refers to spin parallel to the magnetic field, whereas spin down refers to anti-parallel spin. The Γ 's are divided by the cyclotron frequency ω_c for presentation reasons.